Biomedical Physics & Engineering Express

ENDORSED BY IPEM Institute of Physics and Engineering in Medicine

ACCEPTED MANUSCRIPT

Assessment of a commercial EPID dosimetry system to detect radiotherapy treatment errors

To cite this article before publication: Paul James Doolan *et al* 2021 *Biomed. Phys. Eng. Express* in press https://doi.org/10.1088/2057-1976/ac02a5

Assessment of a commercial EPID dosimetry system to detect radiotherapy treatment errors

Author details
Paul Doolan[1*], Maria Nikolaou[1], Konstantinos Ferentinos[2], Georgios Anagnostopoulos[1]
[1]*Department of Medical Physics and Bioengineering, German Oncology Center, Limassol, Cyprus.*
[1]*Department of Radiation Oncology, German Oncology Center, Limassol, Cyprus.*
*Corresponding author: paul.doolan@goc.com.cy

Abstract: One method for detecting radiotherapy treatment errors is to capture the exit dose using an electronic portal imaging device. In comparison with a baseline integrated image, subsequent fractions can be compared and differences in images suggest a difference in the radiation treatment delivered. The aim of this work was to assess the sensitivity of a commercial software PerFRACTION in detecting such differences, arising from three possible sources: (i) changes in the radiation beam or EPID position; (ii) changes in the patient position; and (iii) changes in the patient anatomy. By systematically introducing errors, PerFRACTION was shown to be very sensitive to changes in the radiation beam. Variation in the beam output could be detected within 0.3%, field size within 0.4 mm, collimator rotation within 0.3° and MLC positioning could be verified to within 0.1 mm. EPID misalignment could be detected within 0.3 mm. PerFRACTION was able to detect the mispositioning of an anthropomorphic phantom by 3 mm with static beams, however there was a relative dependency between the patient geometry and the direction of the shift. VMAT beams were less sensitive to patient misalignments, with a shift of 10 mm only detectable once a strict criterion of 1% dose difference was applied. In another simulated scenario PerFRACTION was also able to detect a weight loss equivalent to a 5 mm change in patient separation in VMAT plans and 10 mm in conformal plans. This work showed that the PerFRACTION software could be relied upon to detect potential radiotherapy treatment errors, arising from a variety of sources.

KEY WORDS
EPID, radiotherapy, monitoring, errors

PACS
87.56.-v (equipment for Radiation therapy)
87.55.-x (Radiation treatment in medical physics)

Body of Manuscript

1. Introduction

Medical radiation incidents can have dire and fatal consequences.[1–3] The safe and accurate delivery of radiation therapy requires three components: (i) a high level quality assurance (QA) programme to ensure correct functioning of the LINAC; (ii) pre-treatment verification checks for individual patients, such as independent monitor unit calculation programs and QA measurements; and (iii) *in vivo* dose measurements during the radiation delivery of an individual patient. Compared to the first two components; *in vivo* dosimetry (IVD) is not only

capable of detecting major errors and assessing deviations between the planned and the delivered dose, but it can also record the dose delivered to individual patients and thus fulfils legal requirements.[4]

The use of routine IVD has been recommended since 2006 in the UK, in an annual report from the Chief Medical Officer.[5] Subsequently, The Royal College of Radiographers recommended the implementation of IVD,[6] but barriers obstructing the implementation, such as time and cost, were also identified,. A variety of *in vivo* dosimetry methods exist, but use of the electronic portal imaging device (EPID) is an attractive, non-interventional, method that has experienced a proliferation recently with the increased application of IMRT and VMAT treatment techniques.[4, 7] Among the available tools for the prevention of errors, it has been shown that the EPID is highly effective at detecting errors when utilized on the first day of, and during, treatments.[8, 9] Almost all modern LINACs come equipped with EPIDs, however one of the reasons that EPID-based dosimetry has taken time to become widespread is that the commercial software required to automatically acquire and analyze the images was not available. [4, 10, 11] This is now changing and PerFRACTION (Sun Nuclear Corporation, Melbourne, FL) is one such software option that will be assessed in this work.

PerFRACTION offers the ability of automatic retrieval and analysis of EPID images acquired during treatment fractions. In the version of the software tested in this work (Version 2), a predicted dose map can either originate from a baseline fraction (usually the first fraction) or from the treatment plan. In this work we focus on the first of these; namely on the ability of the system to detect relative errors between fractions. An assessment of the fraction-by-fraction absolute dose will follow in a separate publication.

In daily clinical practice the deployment of the EPID beyond the patient allows for the exit dose to be captured. Any potential change in this exit dose between fractions indicates a potential change in the patient's treatment, which could arise from a number of sources.[12] In this work we investigate changes that could originate from three possible factors: (i) changes in the radiation beam from the machine or EPID misalignment; (ii) changes in the patient position; or (iii) changes in the patient anatomy. This work aims to investigate the sensitivity of a commercial EPID dosimetry system to changes originating from these three error sources.

To date there have been two other studies that also assess the sensitivity of PerFRACTION to changes in the radiation beam, but no studies have investigated the sensitivity to EPID panel misalignment. Zhuang and Olch[13] varied the jaw position, induced MLC leaf position errors, collimator rotation errors and altered the machine output. The major difference with our work is the testing on an Elekta LINAC (Zhuang and Olch tested a TrueBeam Varian LINAC) and the testing of EPID misalignments. Bresciani *et al*[14] performed an investigation on the PerFRACTION sensitivity and detection thresholds (gamma analysis, global passing rate with variable %DD and DTA values) for various VMAT plans by delivering dose to a spherical target inside a thoracic anthropomorphic phantom. They tested machine output modifications, such as single leaf MLC position variations at specific control points. They tested the sensitivity to patient anatomical changes through the removal of 1.25 and 2.5 cm thick bolus material to mimic patient weight loss. In our work we also investigate the sensitivity to

patient anatomic variations through the removal of bolus sheets but look at the impact on 3DCRT (with two different energies) as well as VMAT plans. In the same work, Bresciani *et al*[14] also assessed patient misalignment sensitivity through shifts of the phantom in the anterior-posterior direction. Hseih *et al*[15] delivered 7-field IMRT plans to a phantom and five canine cadaver heads. The sensitivity of PerFRACTION to patient misalignment was assessed by subjecting the cadavers to translational position errors of 1, 3 and 5 mm, with images analyzed using gamma analysis and percentage differences. In our work we shift an anthropomorphic 3D printed head phantom between 1 to 40 mm, and assessed the impact on 3DCRT, IMRT and VMAT plans.

2. Material and methods

2.1. PerFRACTION software

The PerFRACTION software (Version 2.0.4) comprises a dedicated server that is connected to the record and verify system (Mosaiq version 2.6.4, ELEKTA, Stockholm, Sweden) and EPID image database (iView 5.1, ELEKTA Stockholm, Sweden). PerFRACTION automatically retrieves EPID images from the iView database using an automated query retrieve process, after which they are processed. No user interaction is required; all EPID images and logs for each fraction are automatically retrieved and analyzed according to a user-defined protocol.

2.2. Acquisition mode and general analysis

All plans were created using Monaco 5.1 (ELEKTA, Stockholm, Sweden) (details of the plans created can be found in subsections 2.3, 2.4 and 2.5). In Monaco, 3DCRT plans use the Collapsed Cone dose calculation algorithm and IMRT/VMAT plans use Monte Carlo. In PerFRACTION doses are calculated using a Superposition/Convolution algorithm consisting of three steps (fluence calculation within the accelerator head, TERMA calculation from the accelerator head to the patient, and superposition within the patient).

All plans were exported to Mosaiq for delivery and delivered on LINACs with an Elekta Agility head (80 MLCs, each 5 mm in width in the plane of the isocenter). Exit doses were captured using the iView EPID. The iView EPID has an amorphous silicon panel with a resolution of 1024 x 1024 pixels, each with a dimension of 0.4 mm x 0.4 mm, giving an active sensor area of 410 mm x 410 mm. Images were acquired at a fixed SSD of 160 cm. For all plans, integrated images were acquired.

In this study the 2D relative mode of PerFRACTION was assessed, in which one fraction acts as a baseline for future fractions. To ensure that errors are not introduced by LINAC variation or drift throughout the experiment, two images were acquired at the start and one at the end of the experiment as a control. Once the baseline fraction has been selected (usually fraction 1), PerFRACTION automatically compares future deliveries against this delivered dose. In this study gamma analysis[16] and percentage dose difference (DD) comparison methods were utilized.

2.3. Experimental measurements – Radiation beam and EPID misalignment errors

The methodology of Zhuang and Olch[13] was utilized to determine the sensitivity of PerFRACTION to radiation beam errors. This involves the following general procedure. (i) Deliver a standard field (in our case 10 cm x 10 cm), which acts as the baseline image. (ii) Deliver an 'erroneous' field, which has some small alterations compared to the baseline. (iii)

Compare the erroneous image to the baseline using PerFRACTION. (iv) In the gamma analysis tolerance settings, vary either the distance-to-agreement (DTA) or DD tolerance until the gamma passing rate reaches an acceptable value. The acceptable passing rates defined are stated in their corresponding subsections, but was generally 95%. (v) The difference between the tolerance that must be applied to achieve an acceptable passing rate and the magnitude of error introduced is defined as the 'sensitivity' of PerFRACTION, to a given error. The various test situations are described below.

Nominally the 10 x 10 cm square was delivered with 200 MU. To investigate the effect of a change in the output of the machine this was varied with ±0.5%, ±1.0%, ±1.5% MUs. The acquired images were compared with the baseline using the DD method. The DD tolerance had to be increased above the induced error to reach a passing rate above 95%. When comparing the reference image with the erroneous images, the acceptable DD passing rate was defined to be 95%.

The field size was varied symmetrically in size from a 10 x 10 cm beam by ±2 mm, ±4 mm and ±6 mm. The field isocenter remained the same and the individual edges of the field were varied by ±1 mm, ±2 mm and ±3 mm. The acquired images were compared with the baseline using the gamma analysis method, with a constant DD of 1.0% (to remove any small variations in LINAC output between deliveries and ensure that the analysis focuses on the field size error). When comparing the reference image with the erroneous images, the acceptable gamma analysis passing rate was defined to be 95%.

Maintaining a 10 x 10 cm field, the collimator was rotated about the isocenter by ±1º, ±2º, and ±3 º. It is necessary to relate the error introduced by a collimator rotation to a change in the field edge in terms of Cartesian co-ordinates, because the DTA tolerance for gamma analysis tolerances in PerFRACTION is defined in Cartesian co-ordinates. Therefore, rotations of a specific angle θ (in degrees) correspond to a field edge change d defined by equation 1,

$$\boldsymbol{d = 2 \times (1 - \cos \theta)^{1/2} \sin\left(45 - \frac{\theta}{2}\right)} \quad (1)$$

where x is the size of the jaw (the distance from the isocenter to the jaw, in this case 5 cm). The acquired images were compared with the baseline using the gamma analysis method, with a constant DD of 1.0% (to ignore any small variations in LINAC output between deliveries and ensure that the analysis focuses on the collimator rotation error). When comparing the reference image with the erroneous images, the acceptable gamma analysis passing rate was defined to be 99% (higher than the standard 95% because of the very few pixels involved in the change).

The shape of the 10 x 10 cm field was altered by altering the positions of a group of five MLCs in the center of one of the field edges. The positions of the five MLCs were altered by ±1, ±2 and ±3 mm. When comparing the reference image with the erroneous images, the acceptable gamma analysis passing rate was defined to be 99% (higher than the standard 95% because of the very few pixels involved in the change).

The shape of the 10 x 10 cm field was altered by altering the position of a single MLC at the center of one of the field edges. The position of this MLC was varied by ±1, ±2 and ±3 mm. When comparing the reference image with the erroneous images, the acceptable gamma analysis passing rate was defined to be 99% (higher than the standard 95% because of the very few pixels involved in the change).

The 10 x 10 cm field was delivered, with the iView EPID panel misaligned. Given that the position of the iView cannot be controlled digitally by the user, the offsets were measured by a ruler in comparison with the light field. Thus, the iView panel was separately shifted: 2.5 mm, 6.0 mm and 10 mm towards the gantry (G); and 3.0 mm, 6.0 mm and 10.0 mm towards the left-hand side of the patient (B). These distances were measured at the plane of the panel (160 cm SID), but the software makes an analysis at the isocenter. The corresponding shifts at isocenter were thus: 1.6 mm, 3.8 mm and 6.3 mm towards G; and 1.9 mm, 3.8 mm and 6.3 mm towards B. When comparing the reference image with the erroneous images, the acceptable gamma analysis passing rate was defined to be 95%.

2.4. Experimental Measurements – Patient misalignment

To test the impact of patient misalignment an anthropomorphic head phantom was used. The PseudoPatient™ 3D printed head phantom (RTSafe, Athens, Greece) has a realistic patient geometry, with the skull composed of bone equivalent density material. Immobilization and localization of the phantom was achieved using a stereotactic head shell device (UNGER Medizintechnik GmbH, Muehlheim- Kaerlich, Germany).

Plans were created with the isocenter at the base of the skull, so that any misalignments would result in beams passing through different heterogeneities and thus different radiological path lengths. Plans were created with three different treatment techniques: 3DCRT; step-and-shoot IMRT; and VMAT. For the 3DCRT case, four beams were created, with equal weighting, at the four cardinal angles. For the IMRT case, seven equally spaced beams were used (0º, 51º, 102º, 153º, 204º, 255º, 306º). For the VMAT case a single full arc was used. No couch or collimator rotations were used in any of the plans.

Following alignment of the phantom on the LINAC using our clinical standard CBCT brain protocol, baseline EPID images were acquired and tests were made with the phantom shifted from the isocenter. To test the sensitivity to patient misalignment it is not necessary to separately shift in all three directions (i.e. Left-Right, Ant-Post, Sup-Inf). To understand this, it is important to consider that the cause of failure in the 2D analysis is due to dose arriving at the EPID that is different from that delivered on the first fraction. Assuming no radiation beam errors, a different dose will be received if there is a variance in the beam absorption caused by passing through different heterogeneities. Moving in different directions simply changes the anatomy through which the beam passes, which thus changes the beam absorption and the image at the EPID. Therefore, the impact of patient misalignment on the EPID image is dependent on the relative geometry of the patient, the position of the isocenter and the magnitude of the shift. Given the first two are patient-specific, it is only necessary to test different magnitudes of shift, in a single direction. Thus, the phantom was shifted in the Left-Right direction only, by moving the couch by various distances: 1, 3, 5, 10, 20, 30, 40 mm.

Images were analyzed using the gamma method, with a tolerance of 3% / 2 mm and global normalization (in the absence of established guidelines for in vivo EPID monitoring, the AAPM TG-218 guidelines[17] for patient-specific QA were employed).

2.5. Measurements – Patient anatomy variation

One of the most prevalent sites for replanning is the head and neck anatomical region, as patients typically lose weight in the neck region during the course of their treatment[18]. To simulate whether PerFRACTION could detect such a change, a cylindrical PMMA phantom was used and three layers of 5 mm thick bolus (UNGER Medizintechnik GmbH, Muehlheim-Kaerlich, Germany) were fixed to the anterior half, as shown in Figure 1. Layers of bolus were removed to simulate weight loss during treatment of the head and neck region and plans were repeatedly delivered.

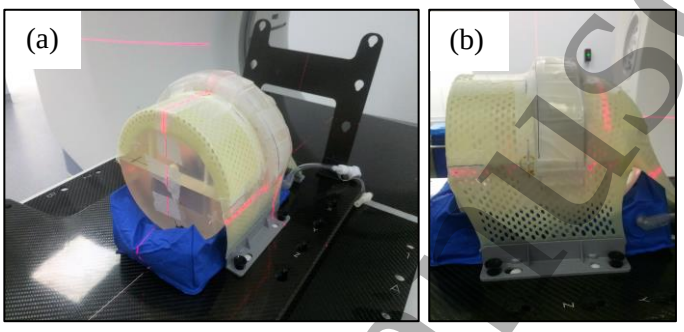

Fig. 1. Cylindrical phantom used for the patient anatomy variation study. (a) A vacuum bag and head and neck shell were used to secure the position of the phantom. (b) Three layers of bolus were added to the anterior of the shell, extending down over the lateral sides.

A variety of plans were created and tested. Plans with a single 3DCRT anterior beam were created, for low (6 MV) and high energy (15 MV) beams. A 3DCRT plan with four equally weighted fields at cardinal angles was created, using 6 MV. A 6 MV VMAT plan was also created, with one full arc. For all four plans dose was directed towards a small, approximately spherical, target in the central anterior region of the cylinder.

Following the acquisition of the baseline image (fraction #1), a single layer of bolus was removed (simulating a weight loss that equates to a change in patient width of 5 mm) and the plan was delivered again (fraction #2). The second and third layers of bolus (fraction #3 and fraction #4) were also removed and the plan was delivered again (simulating weight losses equating to changes in patient widths of 10 and 15 mm, respectively). As the bolus extended over the anterior and lateral parts of the cylinder, in the 3DCRT plan the anterior and posterior fields were subjected to a changes in patient thickness of 5, 10 and 15 mm for the removal of one, two and three layers of bolus, respectively; but the left and right fields were subjected to thickness changes of 10, 20 and 30 mm for the removal of one, two and three layers of bolus, respectively.

3. Results

3.1. Radiation beam and EPID misalignment errors

In Figures 2-7 the impact on the passing rate when a variety of errors were intentionally introduced to the radiation beam is presented. Each row corresponds to a different test; on the left is the graph of gamma passing rates when varying the DTA tolerance; in the center is the 'erroneous' radiation field; and on the right is the gamma difference map when compared to a

standard 10 x 10 cm field. Measurements were also made with the EPID panel shifted longitudinally and laterally by three different magnitudes. Table 1 provides quantitative details of the results, together with the computed sensitivity of PerFRACTION to detect changes to such errors. Each of the errors introduced will be discussed in sections 3.1.1 to 3.1.6.

Table 1. Table of results for radiation beam errors. The magnitude of induced error is listed, together with the dose difference (DD) or distance-to-agreement (DTA) tolerance required to obtain an acceptable passing rate. For a given test, the sensitivity is the largest of these values, which is highlighted with a ***bold and underlined*** *typeface.*

Test	Induced error	Lowest DD [%] or DTA [mm] with acceptable passing rate	PerFRACTION sensitivity
Machine output	+0.5%, -0.5%	0.8%, 0.7%	**0.3%**
	+1.0%, -1.0%	1.2%, 1.0%	0.2%
	+1.5%, -1.5%	1.6%, 1.5%	0.1%
Field size	+1 mm, -1 mm	1.1 mm, 1.2 mm	0.2 mm
	+2 mm, -2 mm	2.2 mm, 2.4 mm	**0.4 mm**
	+3 mm, -3 mm	3.4 mm, 3.4 mm	0.4 mm
Collimator rotation	+1°, -1°, (0.9 mm)	0.8 mm, 0.8 mm	0.1° (0.1 mm)
	+2°, -2°, (1.7 mm)	1.5 mm, 1.5 mm	0.2° (0.2 mm)
	+3°, -3° (2.5 mm)	2.2 mm, 2.2 mm	**0.3°** (0.3 mm)
MLC group	+1 mm, -1 mm	1.0 mm, 1.0 mm	0.0 mm
	+2 mm, -2 mm	2.0 mm, 2.1 mm	0.1 mm
	+3 mm, -3 mm	2.9 mm, 2.9 mm	**0.1 mm**
Single MLC (6X)	+1 mm, -1 mm	0.5 mm, 0.9 mm	0.4 mm
	+2 mm, -2 mm	1.0 mm, 1.9 mm	1.0 mm
	+3 mm, -3 mm	1.9 mm, 3.6 mm	**1.1 mm**
EPID misalignment (GT)	1.6 mm	1.5 mm	0.1 mm
	3.8 mm	3.8 mm	0.0 mm
	6.3 mm	6.0 mm	**0.3 mm**
EPID misalignment (AB)	1.9 mm	2.0 mm	0.1 mm
	3.8 mm	3.6 mm	0.2 mm
	6.3 mm	6.1 mm	0.2 mm

Abbreviations: DD = dose difference; DTA = distance-to-agreement.

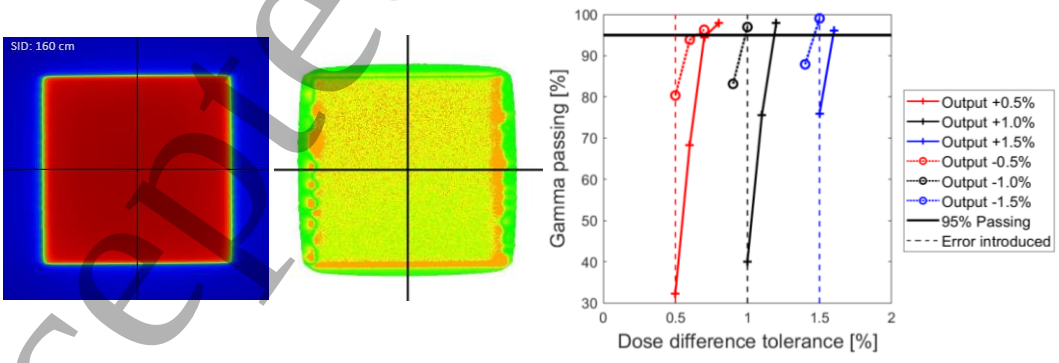

Fig. 2. Results when varying the LINAC output. (Left: erroneous field; centre: gamma map; right gamma passing rates).

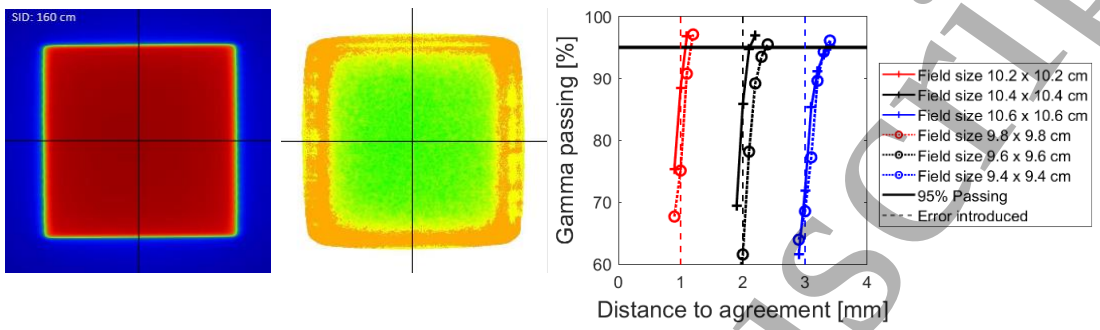

Fig. 3. Results when varying the field size. (Left: erroneous field; centre: gamma map; right gamma passing rates).

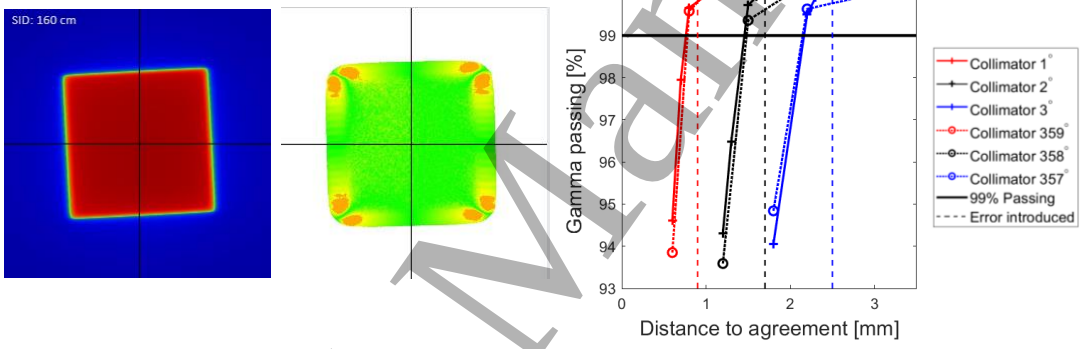

Fig. 4. Results when collimator rotations were applied. (Left: erroneous field; centre: gamma map; right gamma passing rates).

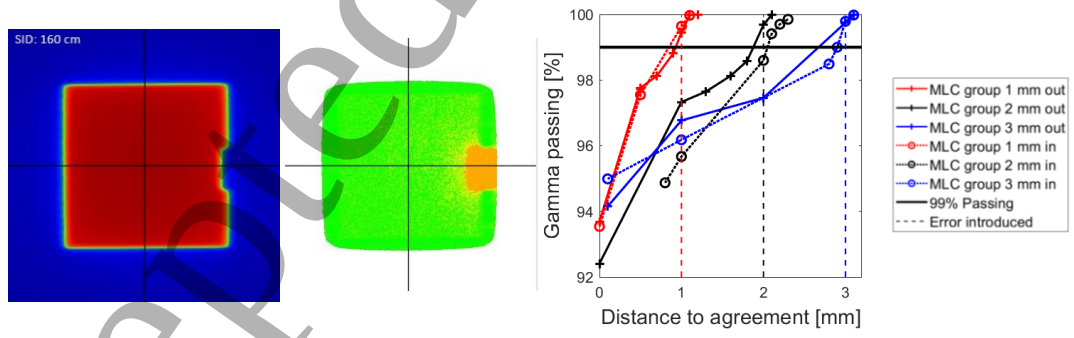

Fig. 5. Results when the position of a group of five MLCs are altered. (Left: erroneous field; centre: gamma map; right gamma passing rates).

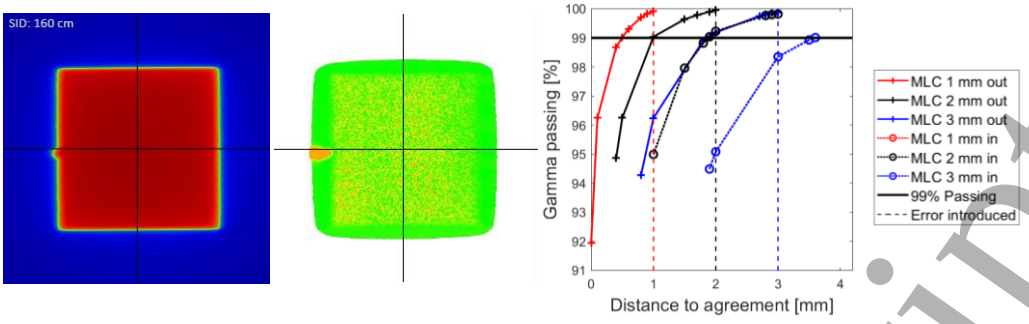

Fig. 6. Results when the position of a single MLC is altered. (Left: erroneous field; centre: gamma map; right gamma passing rates).

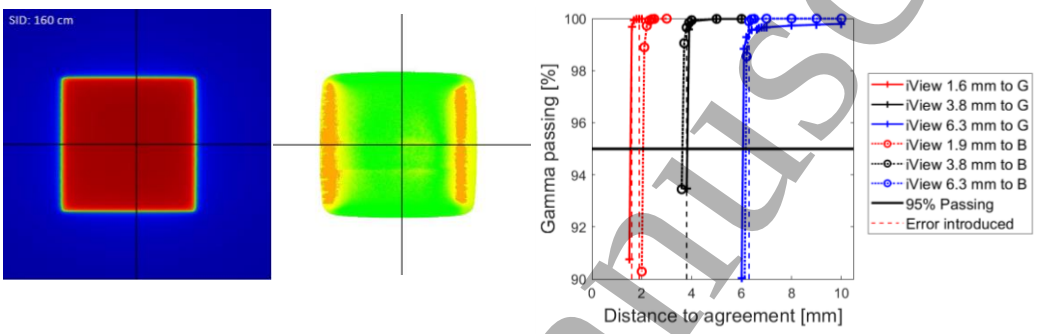

Fig. 7. Results when the iView was misaligned. (Left: erroneous field; centre: gamma map; right gamma passing rates).

Table 1 and Figure 2 show the results when varying the machine output by ±0.5%, ±1.0%, ±1.5%. The sensitivity of PerFRACTION to varying machine output was found to be 0.3%.

Table 1 and Figure 3 show the results when varying the field size by ±2 mm, ±4 mm and ±6 mm. Individual jaws were altered by ±1 mm, ±2 mm and ±3 mm, and the sensitivity of PerFRACTION was found to be 0.4 mm.

Table 1 and Figure 4 show the results when rotating the collimator of the 10 x 10 cm field by ±1º, ±2ºand ±3º. As explained in Section 2.3.3, rotations of ±1º, ±2º and ±3º correspond to maximum changes in the size of the field along one edge of 0.9, 1.7 and 2.5 mm. It was found that the sensitivity of PerFRACTION to rotating the collimator was 0.3 mm, which corresponds to 0.3º for this field size.

Table 1 and Figures 5 and 6 show the results when the MLC shape is varied. In Figure 2(d) the results of varying a group of five MLCs by ±1, ±2 and ±3 mm is shown and in Figure 2(e) are the same shifts of a single MLC. It was found that PerFRACTION was sensitive to within 0.1 mm for a group of MLCs and 1.1 mm for an individual MLC.

Table 1 and Figure 7 show the results when the EPID panel is misaligned. For shifts of 1.6, 1.5 and 6.3 mm in the GT direction and shifts of 1.9, 3.8 and 6.3 mm in the AB direction, PerFRACTION was found to be sensitive to within 0.3 mm.

3.2. Patient misalignment

Table 2 shows the results for the patient misalignment simulation study. As expected, the general trend the gamma passing rate decreases as the lateral shift increases.

In the 3DCRT plan cardinal beams were delivered. The passing rates for the left and right lateral beams remained at 100.0% for a shift of up to 40 mm. However, the passing rates for the anterior and posterior beams were affected for shifts greater than or equal to 3 mm.

For the step-and-shoot IMRT plan, all beams are affected by the lateral shift, but the point at which the passing rate falls below 95% varies for each beam due to the relative geometry between the beam and the patient heterogeneities.

The VMAT plan is unaffected by shifts in the patient of up to 30 mm, when assessed using gamma analysis. To analyze the VMAT plan in more depth, an assessment was made both with gamma analysis with tighter tolerances and using a DD method (i.e. DTA set to zero). The results are shown in Table 3. It can be seen that with a strict DD tolerance of 1%, lateral shifts of 10 mm could be detected.

*Table 2. Table of results for the patient misalignment simulation study. Values are shown for gamma passing rates for a tolerance of 3% / 2 mm. Passing rates with values less than 95% are highlighted in a **bold and underlined** typeface.*

Plan	Field (Angle)	#Fraction (Lateral shift applied)							
		#1 (0 mm)	#2 (1 mm)	#3 (3 mm)	#4 (5 mm)	#5 (10 mm)	#6 (20 mm)	#7 (30 mm)	#8 (40 mm)
3DCRT	Ant (0°)	100.0%	100.0%	**93.4%**	**88.6%**	**75.9%**	**64.8%**	**59.5%**	**60.2%**
	Left (90°)	100.0%	100.0%	100.0%	100.0%	100.0%	100.0%	100.0%	100.0%
	Post (180°)	100.0%	100.0%	**91.8%**	**86.8%**	**76.3%**	**69.6%**	**59.8%**	**60.0%**
	Right (270°)	100.0%	100.0%	100.0%	100.0%	100.0%	100.0%	100.0%	100.0%
IMRT	Ant (0°)	100.0%	99.5%	**94.9%**	**93.2%**	**82.5%**	**72.4%**	**70.9%**	**63.0%**
	LAO (51°)	100.0%	100.0%	96.5%	**94.2%**	**89.6%**	**81.0%**	**76.5%**	**78.6%**
	LPO (102°)	100.0%	100.0%	100.0%	100.0%	100.0%	97.2%	**91.8%**	**91.8%**
	PLO (153°)	100.0%	100.0%	95.2%	**91.1%**	**83.9%**	**77.5%**	**67.4%**	**67.5%**
	PRO (204°)	100.0%	100.0%	99.3%	97.8%	**94.8%**	**86.8%**	**65.6%**	**63.5%**
	RPO (255°)	100.0%	100.0%	100.0%	100.0%	100.0%	96.4%	**87.6%**	**86.4%**
	RAO (306°)	100.0%	100.0%	100.0%	100.0%	97.4%	**94.1%**	**84.6%**	**89.8%**
VMAT	Arc1	100.0%	100.0%	100.0%	100.0%	100.0%	100.0%	100.0%	**90.8%**

*Table 3. Table of results for the patient misalignment simulation study for the VMAT plan, assessed with different gamma analysis tolerances and with different dose differences. Passing rates with values less than 95% are highlighted in a **bold and underlined** typeface.*

Method	Tolerance	#Fraction (Lateral shift applied)							
		#1 (0 mm)	#2 (1 mm)	#3 (3 mm)	#4 (5 mm)	#5 (10 mm)	#6 (20 mm)	#7 (30 mm)	#8 (40 mm)
Gamma	3% / 3 mm	100.0%	100.0%	100.0%	100.0%	100.0%	100.0%	100.0%	**92.9%**
Gamma	3% / 2 mm	100.0%	100.0%	100.0%	100.0%	100.0%	100.0%	100.0%	**90.8%**
Gamma	3% / 1 mm	100.0%	100.0%	100.0%	100.0%	100.0%	100.0%	100.0%	**84.3%**
Gamma	2% / 2 mm	100.0%	100.0%	100.0%	100.0%	100.0%	100.0%	99.3%	**87.7%**
Gamma	2% / 1 mm	100.0%	100.0%	100.0%	100.0%	100.0%	100.0%	96.8%	**78.5%**
Gamma	1% / 1 mm	100.0%	100.0%	100.0%	100.0%	100.0%	99.8%	**89.0%**	**76.0%**
DD	3%	100.0%	100.0%	100.0%	100.0%	100.0%	100.0%	96.5%	**55.2%**
DD	2%	100.0%	100.0%	100.0%	100.0%	100.0%	100.0%	**71.1%**	**37.8%**
DD	1%	100.0%	100.0%	100.0%	98.9%	**90.1%**	**69.5%**	**30.1%**	**17.7%**

Abbreviations: DD = dose difference.

3.3. Patient anatomy variation

Table 4 shows the results for the study that simulates patient weight loss in the head and neck anatomical area. As expected, there is a decrease in the passing rate as more bolus is removed.

*Table 4. Table of results for the patient weight loss simulation study. Values shown are the gamma passing rates for a tolerance of 3% / 2 mm. Passing rates with values less than 95% are highlighted in a **bold and underlined** typeface.*

Plan	Field	#Fraction (Bolus thickness removed)			
		#1 (0 mm)	#2 (5 mm)	#3 (10 mm)	#4 (15 mm)
3DCRT, 6X	Ant	100.0%	100.0%	**58.3%**	**51.6%**
3DCRT, 15X	Ant	100.0%	100.0%	**67.3%**	**55.8%**
3DCRT, Box	Post	100.0%	100.0%	**91.1%**	**52.7%**
	Left	100.0%	**63.8%**	**49.4%**	**41.5%**
	Ant	100.0%	100.0%	**44.2%**	**53.0%**
	Right	100.0%	**72.3%**	**50.8%**	**43.3%**
VMAT	Arc1	100.0%	**94.2%**	**69.5%**	**4.5%**

For the 3DCRT single anterior beams, both 6 MV and 15 MV are equally affected, with very similar passing rates when a specific bolus thickness is removed. Bolus removal of 5 mm is not detected, but the passing rates drop dramatically at 10 mm, and even further 15 mm.

For the 3DCRT four-field box plan, the left and right fields are affected more as the bolus extended over the top half of the cylinder and down the sides. Thus, the lateral fields were subjected to twice the 'weight loss' from either side of the cylinder, and passing rates thus fall when a single 5 mm thickness of bolus is removed. As with the single anterior beam plans, the anterior and posterior fields are unaffected when 5 mm of bolus is removed. Gamma passing rates become progressively worse as subsequent layers of bolus are removed.

The VMAT plan is sensitive to 5 mm of weight loss. Gamma passing rates become progressively worse as subsequent layers of bolus are removed.

4. Discussion

In this work we have investigated the sensitivity of PerFRACTION in detecting errors in radiation therapy treatments, from a variety of sources. It is possible that a mistreatment could occur from an error in the radiation beam, from the patient being misaligned, or if the anatomy of the patient differs from that at the time of the planning CT.

In the commercial software PerFRACTION, it is possible to use integrated images captured during treatments to assess the consistency of treatment. Treatment fractions are compared to the first (baseline) fraction. If the treatment is identical then the images match. If, however, there is an alteration of the radiation beam, the patient position or the patient shape, then the image formed will vary. In this work we systematically investigated the sensitivity of PerFRACTION to detect errors arising from these three separate sources.

4.1. Radiation beam and EPID misalignment errors

In general, PerFRACTION was found to be very sensitive to changes in the radiation beam. The sensitivity of PerFRACTION to varying machine output was found to be 0.3%, which is in close agreement with the results of Zhuang and Olch[13] (0.2%). In the clinical scenario

utilized by Bresciani *et al*,[14] dose output variations to the VMAT plans of 1% or 2% were not detected until a very strict gamma criterion of 1%/1 mm was employed.

In our study it was found that PerFRACTION was sensitive to changes in the field size of 0.4 mm, which agrees well with Zhuang and Olch[13] (0.2 mm). It was found that PerFRACTION was sensitive to collimator rotations of 0.3º, which is also in close agreement with the results of Zhuang and Olch[13] (0.5º).

It was found that the sensitivity of PerFRACTION to detecting the position of a group of five MLCs was 0.1 mm. The ability of the software to detect the mispositioning of a single MLC was more difficult to assess because so few pixels were involved. Using a threshold passing rate of 99%, a single MLC could be detected with a sensitivity of 1.1 mm. The result of Zhuang and Olch[13], which tested a series of single MLCs offset by different magnitudes, lies between these two values, at 0.4 mm.

The sensitivity of PerFRACTION to errors in the alignment of the EPID panel was investigated by delivering a 10 cm x 10 cm radiation field to a misaligned panel and comparing to the image acquired with the EPID in the correct position. For shifts of the EPID panel in the GT and AB directions (for Elekta machines the EPID SSD cannot be adjusted) it was found that the sensitivity of PerFRACTION was 0.3 mm. To date there have been no other works looking into the sensitivity of the system to EPID panel misalignment, but it is encouraging that our result is very similar to our field size sensitivity result.

4.2. Patient misalignment

Using an anthropomorphic head phantom (PseudoPatient™, RTSafe) the sensitivity of PerFRACTION to patient misalignment was tested. It was found that the passing rate significantly decreased if the shift resulted in the beams traversing different heterogeneities than originally planned.

In the four-field 3DCRT plan, the left lateral shifts applied in the study resulted in no change to the heterogeneities traversed by the left and right lateral beams (the magnification of certain structures with the shift was negligible), and thus the passing rates remained at 100%, even with shifts of 40 mm. However, the anterior and posterior beams passed through different anatomy with varying attenuation levels (in the nasal region), and thus the passing rates dropped below 95% for 3 mm shifts.

The same effect was observed for the IMRT plan. Being static step-and-shoot beams (equally-spaced beams at angles of 0º, 51º, 102º, 153º, 204º, 255º, 306º) they are completely dependent on the geometry of the phantom and the shift that is made. The weight of the beam is not important as beams are assessed individually and comparisons are made relative to the first fraction of the beam. Inspection of Table 2 suggests that the Ant (0º), LAO (51º) and PLO (153º) fields are affected most, whereas the LPO (102º) and RPO (255º) fields are most robust to patient shifts in the left direction. These results are in good agreement with those of Hseih *et al*,[15] who also shifted their canine cadaver in a lateral direction. They also delivered a 7-field IMRT plan at the same angles and found that for a shift of 2 cm, using a gamma criterion of 3% / 1 mm, that the Ant (0º), LAO (51º), PLO (153º) and RAO (306º) fields had passing rates below 95%. In agreement with our results, the LPO (102º) and RPO (255º) fields still had high passing rates (both >98%) even for a 2 cm shift.

In our study the VMAT plan was found to be insensitive to misalignments of up to 30 mm when assessed using gamma analysis, which agrees with other studies. Bresciani *et al*[14] found that for an anterior-posterior shift of 11 mm in an anthropomorphic thoracic phantom the 2% / 2 mm global gamma passing rates remained greater than 97.9%. The cause of this 'insensitivity' is hypothesized to be because the higher weighted segments of the arc are directed through gantry angles that are less affected by heterogeneities. As was found in the 3DCRT and IMRT plans, beams that pass through the lateral directions of the plan were much less affected by a lateral shift. As the VMAT plan is not composed of static beams, it is much more difficult to decompose the effect that patient misalignments will have on the result. If the arc is more highly weighted through the lateral directions and less through the anterior and posterior directions, it would be less sensitive to a lateral shift (in this case).

Another possible reason for the passing rates of the VMAT plan being unaffected up to such large patient shifts are that the gamma analysis method masks the differences. It has been demonstrated previously by Bojecko *et al*[19] that 5 or 10 mm positional displacements cannot be readily detected by the gamma index (for their specific patient cohort), with Kruse[20] also finding that per-field gamma analysis is a poor predictor of dosimetric accuracy. As found by Hsieh *et al*,[15] the use of the DD method is more sensitive to differences in the image as the DTA component of the gamma analysis is not "masking errors in the gradient-rich fluence of individual IMRT fields". In our study we also found the DD to be more sensitive. With a 2% DD tolerance 30 mm shifts were detected; and with a 1% DD shifts of 10 mm were detected. It is concluded that PerFRACTION can be reasonably sensitive to patient misalignments, provided the DD method is used.

Given that the standard of care for many anatomical sites is now IMRT or VMAT, the authors recommend that EPID dosimetry not be relied upon to confirm the correct patient position, which is consistent with many other studies.[19, 21–23] Gamma analysis masks the differences, and even using a DD comparison method with a 1% tolerance does not allow shifts of <10 mm to be detected. Daily CBCT imaging is considered more suitable for this purpose.

4.3. Patient anatomy variation

It is well known that patients receiving radiotherapy in the head and neck region experience significant anatomic changes during their treatment course.[18] This includes the shrinking of the primary tumor, postoperative changes and edema, and changes in overall body weight. To simulate this neck weight loss, layers of bolus were removed from the surface of a cylindrical PMMA phantom. Conformal 3DCRT and VMAT plans were used to test the sensitivity of PerFRACTION to detect such weight loss.

For conformal plans a weight loss of 5 mm was undetected, but a weight loss of 10 mm led to a drop in the global gamma passing rate to as low as 44.2%, when using a 3% / 2 mm criterion. PerFRACTION was more sensitive in the VMAT case however, with a weight loss of 5 mm leading to a drop in the global gamma passing rate below 95%. This is an important result as head and neck tumors are commonly treated using VMAT techniques. In a similar study using an anthropomorphic phantom, Bresciani *et al*[14] reported that the removal of 1.25 cm of bolus was only detectable with a strict 1% / 1 mm criterion (64.8% passing rate), while for a 2% / 2 mm criterion the passing rate was 99.1%. Hence, we conclude that for different anatomical regions and different VMAT plans, there could be a large variety in the detection

threshold of potential anatomical changes due to weight loss. However, if there is a change to be detected, PerFRACTION is sufficiently sensitive to locate it.

5. Conclusion

In this work we have systematically investigated the sensitivity of the commercial software PerFRACTION to detect radiotherapy treatment errors. Integrated EPID images formed from the exit dose of erroneous treatment fractions were compared to a baseline and assessed using a DD or 2D gamma analysis method. It was found that PerFRACTION was highly sensitive to changes in the radiation beam such as the beam output (0.3%), field size (0.4 mm), collimator rotation (0.3°) or MLC positioning (0.1 mm), as well as EPID panel mispositioning (0.3 mm). Changes in the patient positioning (3 mm) could be detected by PerFRACTION, provided static beams were used and provided the misalignment led to a change in the anatomical heterogeneity through which the beam passed. VMAT beams were less sensitive to patient misalignments; a 10 mm shift could only be detected when using a very strict criterion of 1% with the DD method. The authors recommend that daily CBCT imaging be relied upon to confirm correct patient alignment. PerFRACTION was also able to detect changes in patient anatomy, with VMAT and 3DCRT plans detecting weight losses of 5 mm and 10 mm, respectively. By systematically testing scenarios according to errors from the three sources (radiation beam; patient misalignment; patient anatomy change), we have demonstrated that PerFRACTION is a sensitive tool for detecting radiotherapy errors.

Acknowledgements

The authors would like to acknowledge the support of Sun Nuclear Corporation, in particular Lukasz Wlodarczyk, who helped to resolve many technical problems; the other German Oncology Center physics team members, Yiannis Roussakis, George Antorkas, George Komisopoulos and Leonidas Georgiou, who contributed to the clinical implementation of PerFRACTION; and German Oncology Center radiation technologist Melka Benjamin, who assisted in experimental measurements. We would also like to gratefully thank RTSafe for providing the PseudoPatient™ 3D printed head phantom and the Medical Physics Laboratory of the University of Athens for providing us the cylindrical PMMA phantom.

References

1 Williams M V. Radiotherapy Near Misses, Incidents and Errors: Radiotherapy Incident at Glasgow. Clin. Oncol. 2007; **19**(1): 1–3.

2 Derreumaux S. Lessons from recent accidents in radiation therapy in France. Radiat. Prot. Dosimetry 2008; **131**(1): 130–135.

3 International Commission on Radiological Protection. *ICRP Publication 112: Preventing accidental exposures from new external beam radiation therapy technologies* (2009).

4 Mijnheer B, Beddar S, Izewska J, Reft C. In vivo dosimetry in external beam radiotherapy. Med. Phys. 2013; **40**(7): 1–19.

5 Department of Health. *On The State of Public Health: Annual Report of the Chief Medical Officer 2005* (2006).

6 British Institute of Radiology. *Implementing in vivo dosimetry* (2008).

7 van Elmpt W, McDermott L, Nijsten S, Wendling M, Lambin P, Mijnheer B. A literature review of electronic portal imaging for radiotherapy dosimetry. Radiother. Oncol. 2008; **88**(3): 289–309.

[8] Ford EC, Terezakis S, Souranis A, Harris K, Gay H, Mutic S. Quality control quantification (QCQ): A tool to measure the value of quality control checks in radiation oncology. Int. J. Radiat. Oncol. Biol. Phys. 2012; **84**(3): e263–e269.

[9] Bojechko C, Phillps M, Kalet A, Ford EC. A quantification of the effectiveness of EPID dosimetry and software-based plan verification systems in detecting incidents in radiotherapy. Med. Phys. 2015; **42**(9): 5363–5369.

[10] MacDougall ND, Graveling M, Hansen VN, Brownsword K, Morgan A. In vivo dosimetry in UK external beam radiotherapy: Current and future usage. Br. J. Radiol. 2017; **90**(1072): 1–14.

[11] Mans A, Wendling M, McDermott LN, et al. Catching errors with in vivo EPID dosimetry. Med. Phys. 2010; **37**(6): 2638–2644.

[12] Bojechko C, Ford EC. Quantifying the performance of in vivo portal dosimetry in detecting four types of treatment parameter variations. Med. Phys. 2015; **42**(12): 6912–6918.

[13] Zhuang AH, Olch AJ. Sensitivity study of an automated system for daily patient QA using EPID exit dose images. J. Appl. Clin. Med. Phys. 2018; (December 2017): 1–11.

[14] Bresciani S, Poli M, Miranti A, et al. Comparison of two different EPID-based solutions performing pretreatment quality assurance: 2D portal dosimetry versus 3D forward projection method. Phys. Medica 2018; **52**(June): 65–71.

[15] Hsieh ES, Hansen KS, Kent MS, Saini S, Dieterich S. Can a commercially available EPID dosimetry system detect small daily patient setup errors for cranial IMRT/SRS? Pract. Radiat. Oncol. 2017; **7**(4): e283–e290.

[16] Low D, Harms W, Mutic S, Purdy J. A technique for the quantitative evaluation of dose distributions. Med. Phys. 1998; **25**(5): 656–61.

[17] Miften M, Olch A, Mihailidis D, et al. Tolerance limits and methodologies for IMRT measurement-based verification QA: Recommendations of AAPM Task Group No. 218. Med. Phys. 2018; **45**(4): e53–e83.

[18] Barker JL, Garden AS, Ang KK, et al. Quantification of volumetric and geometric changes occurring during fractionated radiotherapy for head-and-neck cancer using an integrated CT/linear accelerator system. Int. J. Radiat. Oncol. Biol. Phys. 2004; **59**(4): 960–970.

[19] Bojechko C, Ford EC. Quantifying the performance of in vivo portal dosimetry in detecting four types of treatment parameter variations. Med. Phys. 2015; **42**(12): 6912–6918.

[20] Kruse JJ. On the insensitivity of single field planar dosimetry to IMRT inaccuracies. Med. Phys. 2010; **37**(6): 2516–2524.

[21] Mijnheer B, Jomehzadeh A, González P, et al. Error detection during VMAT delivery using EPID-based 3D transit dosimetry. Phys. Medica 2018; **54**(September): 137–145.

[22] Bedford JL, Hanson IM, Hansen VN. Comparison of forward- and back-projection in vivo EPID dosimetry for VMAT treatment of the prostate. Phys. Med. Biol. 2018; **63**(2).

[23] Olaciregui-Ruiz I, Rozendaal R, Mijnheer B, Mans A. Site-specific alert criteria to detect patient-related errors with 3D EPID transit dosimetry. Med. Phys. 2019; **46**(1): 45–55.